Chemistry and Physics of Lipids 218 (2019) 40–46

Contents lists available at ScienceDirect

Chemistry and Physics of Lipids

journal homepage: www.elsevier.com/locate/chemphyslip

The interaction of lipid-liganded gold clusters (Aurora™) with lipid bilayers

Jesús Sot[a,b,1], Sebastião A. Mendanha-Neto[c,1], Jon V. Busto[a], Aritz B. García-Arribas[a], Shengrong Li[d], Stephen W. Burgess[d], Walt A. Shaw[d], David Gil-Carton[e], Félix M. Goñi[a,b], Alicia Alonso[a,b,*]

[a] Instituto Biofisika (UPV/EHU, CSIC), Barrio Sarriena s/n, 48940, Leioa, Spain
[b] Departamento de Bioquímica y Biología Molecular, Universidad del País Vasco, Barrio Sarriena s/n, 48940, Leioa, Spain
[c] Institute of Physics, Federal University of Goiás, Goiás, Brazil
[d] Avanti Polar Lipids, Alabaster, Alabama, USA
[e] Structural Biology Unit, Center for Cooperative Research in Biosciences, CIC bioGUNE, Derio, Spain

ARTICLE INFO

Keywords:
Lipid-liganded gold clusters
Aurora™
lipid bilayers
Lipid phases
Atomic force microscopy

ABSTRACT

Lipid bilayers of different phospholipid compositions have been prepared, in the form of vesicles, or of supported lipid bilayers, and doped with Aurora™ at 0.1 mol%. Aurora™ consists of an Au_{55} gold nanoparticle (about 1.4 nm in diameter) capped with triphenylphosphine ligands and a single diglyceride (distearoyl glycerol) ligand. Gold nanoparticles have been incorporated in the past inside liposomes, or grafted onto their surfaces, with diagnostic or therapeutic aims. Including the gold nanoparticles in a stable form within the lipid bilayers has serious technical difficulties. We have tested the hypothesis that, because of the diglyceride ligand, Aurora™ would allow the easy incorporation of gold nanoclusters into cell membranes or lipid bilayers. Our results show that Aurora™ readily incorporates into lipid bilayers, particularly when they are in the fluid phase, i.e. the state in which cell membranes exist. Calorimetric, fluorescence polarization or fluorescence confocal microscopy concur in showing that bilayer-embedded Aurora™ hardly changes the physical properties of the bilayers, nor does it perturb the phase equilibrium in lipid mixtures giving rise to lateral phase separation in the plane of the membrane. Atomic force microscopy shows, in fluid bilayers, well-resolved particles, 1.2–2.9 nm in height, that are interpreted as single Aurora™ conjugates. Cryo-transmission electron microscopy allows the clear observation of lipid bilayers with an enhanced contrast due to the Aurora™ gold nanoparticles; the single particles can be resolved at high magnification. Our studies support the applicability of Aurora™ as a membrane-friendly form of nano-gold particles for biological research or clinical applications.

1. Introduction

Au_{55} cluster nanoparticles (Schmid et al., 2000a; Schmid and Simon, 2005; Schmid, 2008) are cubo-octahedral structures, 1.4 nm in size, belonging to the family of the so-called full-shell clusters, particles with perfectly completed geometries. These clusters are singular in allowing single-electron switching at room temperature. Gold nanoparticles are also notorious by their self-assembly characteristics, e.g. in the presence of thiol groups (Schmid, 2008; Schmid et al., 2000b; Balasubramanian et al., 2005). Au_{55} clusters show an unusual cytotoxicity, apparently due to their interaction with the major grooves of DNA. In spite of it, a variety of technologies has been developed to introduce gold nanoparticles in living cells and even whole animals (Li et al., 2015; Murphy et al., 2008; Marchesano et al., 2013). Biocompatibility of these particles has been correlated with their endocytotic fate inside the cellular compartment (Shukla et al., 2005; Schmid et al., 2017). Particle surface functionalization with polyoxometalates and lysine can be used to fine-tune their antimicrobial properties (Daima et al., 2013). Gold nanoparticles have been functionalized as nanozymes for kanamycin detection using aptamers (Sharma et al., 2014). Moreover the antitumor effects of doxorubicin in two human cervical tumor cell lines have been potentiated by gold nanoparticles (Tomoaia et al., 2015).

Several preparations of gold nanoparticles associated with membrane lipids are now available, and this opens the way for their use as membrane probes or labels. Walker et al. (2018) have used 1.6-nm gold particles bound to dipalmitoyl phosphatidylethanolamine to examine the viscoelastic and permeability properties of fungal cell walls in

* Corresponding author.
E-mail address: felix.goni@ehu.es (A. Alonso).
[1] Co-first authors.

https://doi.org/10.1016/j.chemphyslip.2018.11.007
Received 21 November 2018; Received in revised form 26 November 2018; Accepted 26 November 2018
Available online 28 November 2018

Candida and *Cryptococcus* species. The preparation of complexes of liposomes with gold nanoparticles has been described (Kojima et al., 2008; Leung and Romanowski, 2012). Aurora™ is a conjugate consisting of a gold cluster capped with triphenylphosphine ligands and a single diglyceride (distearoyl glycerol) ligand (Avanti Polar Lipids catalog, 2018). In this contribution we intend to describe the interactions of Aurora with lipid bilayers of different biophysical properties, and explore its potential applications to membrane biology studies. A variety of microscopic techniques (confocal, atomic force and cryo-TEM) demonstrate the incorporation of Aurora™ into laterally-homogeneous and –heterogeneous bilayers, and a number of subtle, if significant, nanoparticle-induced changes in the bilayer properties. Our results show that Aurora™ can be used in the visualization of lipid bilayers by electron microscopy, and can also become an atomic ruler in AFM studies of supported lipid bilayers.

2. Materials and methods

2.1. Chemicals

The lipids 1-palmitoyl-2-oleoyl-sn-glycero-3-phosphocholine (POPC), 1,2-dioleoyl-sn-glycero-3-phosphocholine (DOPC), 1,2-distearoyl-sn-glycero-3-phosphocholine (DSPC), N-palmitoyl-D-erythro-sphingosylphosphorylcholine (PSM), 1,2-dipalmitoyl-sn-glycero-3-phosphocholine (DPPC), the fluorescent probe 1,2-dipalmitoyl-sn-glycero-3-phosphoethanolamine-N-(lissamine rhodamine B sulfonyl) (Liss-Rho-PE), cholesterol (chol) and 1,2-distearoyl-sn-glycero-3-(Au_{55} nanoparticles) (Aurora™) were supplied by Avanti Polar Lipids Inc. (Alabaster, USA). The fluorescent probe 1,6-diphenyl-1,3,5-hexatriene (DPH) was purchased from Molecular Probes (Eugene, USA). All other reagents were of analytical quality and all solutions were prepared with Milli-Q water (Chart 1).

2.2. Aurora manipulation

Aurora™ particles were characterized using a variety of physical techniques. The mass spectrum of the lipid moiety is shown in Fig. S1. Particle size distribution, UV and IR spectra of the particles are shown respectively in Fig. S2 A, B, and C.

Films containing Aurora™ dissolved in chloroform (0.5 mg/mL) were formed in PFA tubes (Savillex, Eden Prairie, USA) by solvent evaporation using a stream of nitrogen gas. The tubes containing the Aurora™ films were stored at 4 °C until their use.

2.3. Giant unilamellar vesicle preparation

Giant unilamellar vesicles (GUV) were prepared by electroformation on a pair of platinum (Pt) wires by a method first developed by (Angelova and Dimitrov (1986); Dimitrov and Angelova, 1988), modified as described previously (20). GUVs were formed in a PRETGUV 3 chamber supplied by Industrias Técnicas ITC (Bilbao, Spain), that allows direct visualization under the microscope, as described in (Montes et al., 2010). A brief summary of the protocol follows: 5 µL of lipid stock solutions (0.2 mM) dissolved in chloroform:methanol (2:1 v/v) containing 0.3 mol% of the fluorescent probe Liss-Rho-PE were added on the surface of platinum electrodes of the formation chambers. The chambers were kept under moderate vacuum during 90 min to remove residual organic solvent. Then, was added 400 µL of buffer (20 mM PIPES, 150 mM NaCl, 1 mM EDTA, pH 7.4) to each chamber and these were connected to an alternating current electric generator TG330 (Thurlby Thandar Instruments, Huntington UK). The parameters of the electroforming process were: frequency of the alternating current, 500 Hz; AC voltage, 0.03 V during 6 min, 0.33 V during 20 min and 0.8 V during 90 min. The chambers were maintained at 60 °C during the electroforming process. The incorporation of Aurora in the samples was performed by addition of the lipid stock solutions in the Aurora films previously prepared. The resulting solutions were gently shaken during 2 min before being added to the platinum electrodes. The final concentration of Aurora in each sample was 0.1 mol%.

2.4. Confocal microscopy

After the formation period, the chambers were introduced in a confocal inverted microscope Nikon D-ECLIPSE C1 (Nikon Inc., Melville, USA) for fluorescence imaging of the GUVs. The excitation wavelength for Liss-Rho-PE was 561 nm. Images were acquired using a detection channel equipped with a filter of 593 ± 20 nm, and treated with the EZ-C1 3.20 (Nikon Inc.) software. All images were acquired at room temperature and no difference in size, formation or distribution of lipid domains was observed during or after the excitation laser exposure.

2.5. Supported planar bilayer preparation

The planar supported bilayers (SPBs) were prepared by the method of adsorption of small unilamellar vesicles (SUVs) (Fidorra et al., 2006; McConnell et al., 1986). Films of lipids dissolved in chloroform:methanol (2:1) was formed in PFA tubes (Savillex, Eden Prairie, USA) by solvent evaporation using a stream of nitrogen gas. The tubes were kept under moderate vacuum during 90 min to remove residual organic solvent and subsequently hydrated with 100 µL of buffer (20 mM PIPES, 150 mM NaCl, 1 mM EDTA, pH 7.4) at 45 °C. The SUVs were formed by sonication of the MLVs suspension during 60 min at 45 °C. Soon after, 60 µL of the SUV suspension was added to a mica substrate (Asheville-Schoonmaker Mica Co., Newport News, USA) previously introduced in a special cell (*BioCell*) for atomic force liquid samples (JPK Instruments microscopy Berlin, Germany). Then, were added to the *BioCell* 60 µL of PIPES buffer containing $CaCl_2$ and 60 µL of PIPES buffer without $CaCl_2$. Finally, the final solution was slowly heated to 45 °C (1 °C/min). The final lipid concentration was 0.17 mM.

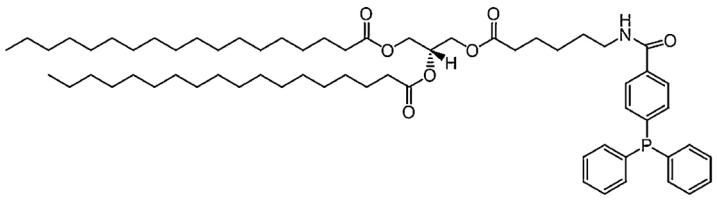

Chemical Formula: $C_{64}H_{100}NO_7P$
Exact Mass: 1025.724
Molecular Weight: 1026.478
m/z: 1025.724 (100.0%), 1026.727 (69.2%), 1027.730 (23.6%), 1028.734 (5.3%), 1027.728 (1.4%), 1026.730 (1.2%)
Elemental Analysis: C, 74.89; H, 9.82; N, 1.36; O, 10.91; P, 3.02

Chart 1. Formula and chemical data for 18:0, 18:0, 6:0 benzyl TG diphenyl phosphine, the derivatized lipid moiety that is complexed to the gold particle for Aurora™ preparation.

After 30 min at 45 °C the *BioCell* temperature was adjusted to room temperature (22–24 °C) and SPBs were equilibrated at this temperature during 30 min. The non adsorbed SUV's were eliminated by PIPES buffer (without $CaCl_2$) exchanges. The incorporation of AURORA in the samples was performed by the addition of lipid stock solutions on the AURORA films previously prepared. The resulting solutions were gently shaken during 2 min before being evaporated by the nitrogen gas flow and the preparation of SUVs was performed as described above. The final concentration of AURORA in each sample was 0.1 mol%.

2.6. Atomic force microscopy

The atomic force microscopy (AFM) experiments were performed on a NanoWizard II (JPK Instruments, Berlin, Germany) microscope equipped with cantilevers and silicon nitride tips (nominal radius ~ 20 nm) model MLCT (Bruker AFM Probes, Camarillo, USA). The spring constant value used in contact mode measurements (vertical deflection of the cantilever constant) was 0.1-0.5 N/m. The images measuring 512 × 512 pixels were acquired at a scan rate of 1 Hz (30 × 30-10 x 10 μM) or 10 Hz (0.5 x 0.5 μM) and treated with JPK Data Processing software (JPK Instruments).

2.7. Multilamellar vesicle preparation

Films of lipids dissolved in chloroform: methanol (2:1) containing 0.2 mol% of the fluorescent probe DPH were formed in PFA tubes (Savillex, Eden Prairie, USA) by solvent evaporation using a stream of nitrogen gas. The tubes were kept under moderate vacuum during 90 min to remove residual organic solvent and subsequently hydrated with 1000 μL of buffer (20 mM PIPES, 150 mM NaCl, 1 mM EDTA, pH 7.4) at 45 °C to form an suspension of multilamellar vesicles (MLVs). The samples were homogenised by sonication at 50 °C during 6 min in a sonicator FB-15049 (Fisher Scientific, Waltham, USA). The incorporation of AURORA in the samples was performed by the addition of lipid stock solutions on the AURORA films previously prepared. The resulting solutions were gently shaken during 2 min before being evaporated by the nitrogen gas flow and the preparation of MLV was performed as described above. The estimated final concentration of AURORA in each sample was 0.1 mol%.

Note that we do not have a feasible assay for AURORA that would allow us to obtain the real AURORA:lipid ratio in our systems. Instead we have operated on the basis of the use of fluorescent probes in membrane studies. It is common practice in those studies to add probes at a nominal lipid:probe ratio similar to our Aurora:lipid ratio. Since these probes are usually hydrophobic (note that Aurora is dispersed in chloroform) they are assumed to be fully incorporated into the bilayer without further experimental quantification, and the same assumption has been made here. Since we have, along the years, confirmed that under our conditions > 95% of the lipids are incorporated into vesicles, this would mean that in the present case it can be safely assumed that the real Aurora:lipid ratio in the bilayers is close to 0.1 mol%, and not above that value.

2.8. Fluorescence anisotropy measurements

Fluorescence anisotropy measurements were performed using a QuantaMaster 40 spectrofluorometer (Photon Technology International, Lawrenceville, USA) with polarizers in the excitation and emission channels and equipped with type L measurement system. A thermal TC125 controller (Quantum Northwest, Liberty Lake, USA) was used to stabilize the sample temperature at 22 °C. The wavelengths of excitation and emission for DPH were 360 and 427 nm respectively. The fluorescence anisotropy was calculated according to the equation.

$$r = \frac{I_{\parallel} - I_{\perp}}{I_{\parallel} + 2I_{\perp}}$$

Where r is the steady-state fluorescence anisotropy and $I_{\parallel}$ and $I_{\perp}$ are the intensities of fluorescence parallel and perpendicular respectively to the polarization plane of the DPH excitation wavelength. Only when anisotropy values remained constant with further dilution were they recorded.

2.9. Cryo-electron microscopy

Samples containing POPC MLVs, with or without 0.1% AURORA were prepared for cryo-EM study. Three microliters of the sample were placed onto 300-mesh R2/1 holey carbon grids (Quantifoil® Micro Tools GmbH, Jena, Germany) and frozen-hydrated following standard methods for cryo-EM, using a Vitrobot Mark III (FEI). Vitrified grids were viewed at liquid nitrogen temperature on a JEM-2000FS/CR field emission gun transmission electron microscope (Jeol Europe, Croissy-sur-Seine, France) operated at 200-kV. An in-column energy filter (Omega filter) produced images with improved contrast and signal to noise ratio. The energy slit width of the energy filter was set up at 30 eV. Digital micrographs were recorded on an Ultrascan4000™ cooled 4 K x 4 K CCD camera (Gatan, Inc) and under low-dose conditions (~30 e-/Å^2) using DigitalMicrograph™ (Gatan, Inc) software. The samples were observed at nominal magnifications of 50,000x and 60,000x resulting in final samplings of 1.8 and 1.3 Å/pixel respectively, and with a defocus range from -1 to −3 μm.

3. Results

The lipid bilayers considered in the present study are either homogeneous: POPC, pSM, DPPC and pSM:Chol (6:4 mol ratio), or laterally heterogeneous: DOPC:DSPC (1:1 mol ratio) and DOPC:pSM:Chol (2:1:1 mol ratio). At room temperature samples containing pure POPC in the fluid-disordered (l_d) phase, those formed by pure pSM or DPPC are in the gel (l_β) phase and the ones composed of pSM:Chol (6:4 mol ratio) are in the fluid-ordered (l_o) phase. Among the heterogeneous bilayers, DOPC:DSPC (1:1 mol ratio) gives rise to a DOPC-rich l_d and a DSPC-rich l_β phase, in turn samples containing DOPC:pSM:Chol (2:1:1 mol ratio) exhibit coexisting DOPC-rich l_d and pSM:Chol-rich l_o phases (Goñi et al., 2008; Collado et al., 2005).

3.1. Confocal microscopy

GUV of the compositions described above were doped with Liss-Rho-PE, that partitions preferentially into the fluid l_d phase (Sot et al., 2008), and examined by confocal fluorescence microscopy (Fig. 1 and Fig. S3). Thus the non-stained zones in each image represent the domains in the l_β or l_o phases. Note that addition of 0.1 mol % Aurora does not modify the vesicle morphology, i.e. it does not generate phase separation in homogeneous samples, nor does it change the structure of pre-existing domains in the heterogeneous ones. The confocal microscopy data confirm the above AFM predictions about phase structure of the various samples.

3.2. Atomic force microscopy

Bilayers of the above compositions were extended over mica and the resulting SPB were examined by AFM. Fig. 2 and Fig. S4 show representative images of bilayers composed of POPC, DPPC, DOPC: DSPC (1:1) and DOPC:pSM:Chol (2:1:1). Adding 0.1 mol% Aurora ™ causes particularly marked changes in the morphology of DOPC:pSM:Chol bilayers, in which Aurora incorporation makes the L_o domains to appear smaller and with not so smooth boundaries. In addition, the difference in bilayer thickness between the (higher) less fluid and (lower) more fluid components in heterogeneous bilayers decreases in the presence of Aurora™ for DOPC:pSM:Chol bilayers, but not for DOPC:DSPC ones (Table S1). The absolute values of bilayer thicknesses can be seen in Table S2. Note that the significant difference in relative

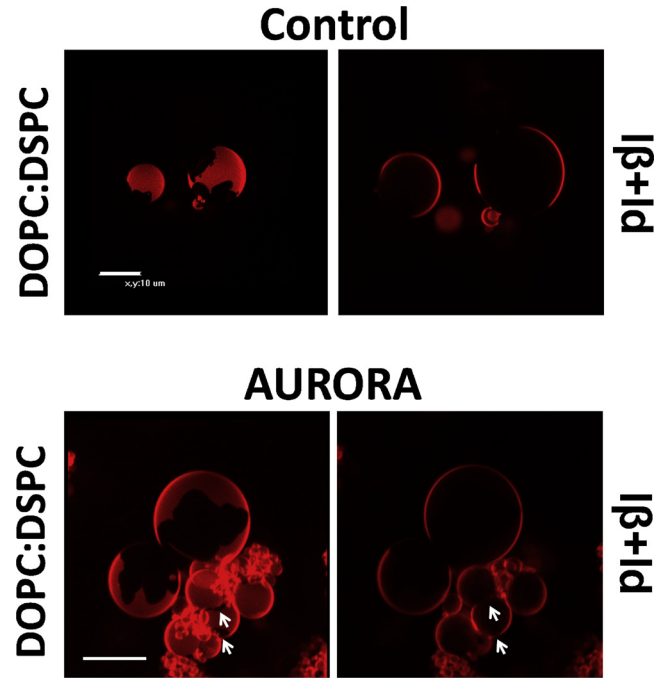

Fig. 1. Confocal fluorescence microscopy of giant unilamellar vesicles of equimolar DOPC:DSPC composition. Representative images. Samples were stained with Lissamine-Rh-PE, a dye that is considered to partition referentially into liquid-disordered phases. The predominant phases are stated at the right hand of the pictures. The four images correspond, respectively from left to right, to: control, 3-dimensional; control, equatorial sections; + Aurora™, 3-dimensional; + Aurora™, equatorial sections. Bars: 20 µm.

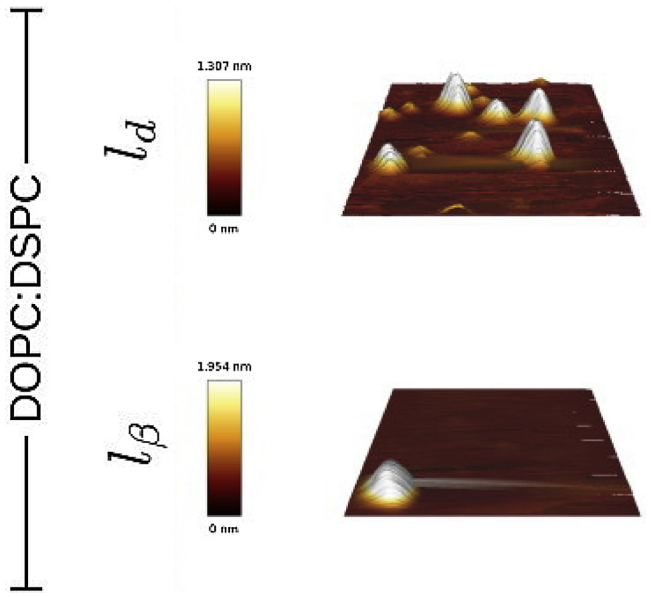

Fig. 3. Imaging the Aurora™ particles by atomic force microscopy. Samples as in Fig. 2. Bilayer areas of 0.5 x 0.5 µm were scanned at 10 Hz. In the DOPC:DSPC sample, areas in both l_d (top) and $l_ß$ (bottom) phases were scanned. A side-view is used to facilitate observation of the embedded particles.

thickness that was seen in DOPC:pSM:Chol bilayers is also detected when the absolute values of the fluid phase (where Aurora™ should be located) are compared. Table S2 also shows that, except for the case just mentioned, Aurora has no other effects on bilayer thicknesses. The observed Aurora effect could be attributed to its interaction with SM, or with SM:Chol domains. Moreover the presence of Aurora in the SUV hampers bilayer extension and causes formation of lipid aggregates. The latter effect is particularly evident in the pure pSM:Chol samples, for which no SPB could be obtained in the presence of Aurora (data not shown). This effect is not only due to the high molecular order of pSM bilayers, since for DPPC samples, exhibiting a similar degree of order, good extensions were achieved also in the presence of Aurora. Rather some phenomenon of preferential SM-Aurora interaction might be occurring for which we do not have an explanation at present.

In order to visualize the Aurora nanoparticles inserted in the SPB and study their behaviour 0.5 x 0.5 µm AFM images were taken from all samples with which a satisfactory spreading had been obtained. In these images small regions of a larger height are consistently observed in the presence, but not in the absence, of Aurora (Fig. 3 and Fig. S5). A larger number of events (Aurora particles or aggregates) are detected in SPB in the fluid phases (l_d or l_o). Because of the hemispherical/conical shape found for the nanoparticles, estimating their real diameter is not trivial. To minimize errors, the average diameter of each particle was considered to be the diameter at mid-height as seen from the transversal sections of the images. Fig. S6 shows the height distributions of the Aurora nanoparticles as a function of their average diameters (the latter obtained using the JPK Data Processing software). Note that for the DOPC:pSM:Chol bilayers reproducible results could only be obtained for the DOPC-rich, l_d domains.

The linear relationship between mean diameter and height of the nanoparticles indicates that Aurora are embedded into the bilayers at different depths but with the same orientation. This suggests that the observed events correspond to single Aurora particles, since particle aggregates would presumably have an irregular shape. The best linear relationships are found for membranes in the l_d phase. The dispersion of experimental points (lack of linearity) in the gel phases could be related to heterogeneous Aurora orientations or to nanoparticles clustering, in turn related to the low fluidity of the gel phase. Note that mean diameter estimations are subject to some intrinsic error, because the heights of both SPB and the particles depend partly on the force exerted by the AFM tips during image acquisition. Unfortunately this force is not completely constant through the different experiments, its adjustment being required to improve image quality.

A more reliable method for measuring the apparent particle size involves measuring the maximum height with respect to the bilayer. In this case the data are not affected by small variations in the force of the AFM tip and can be obtained from the same images as shown in Fig. S5 (right hand column). The vast majority of the particles remained stable

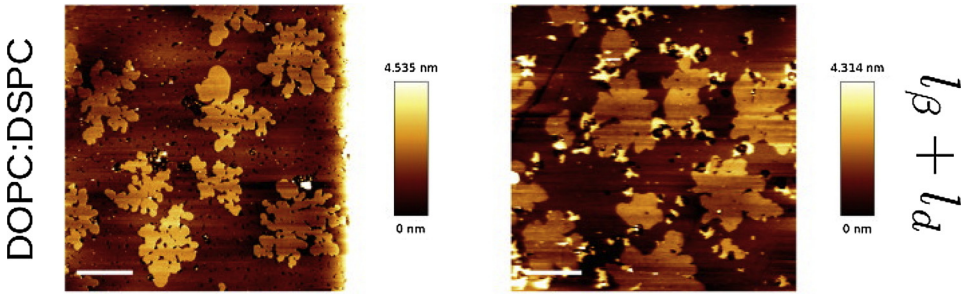

Fig. 2. Atomic force microscopy of supported lipid bilayers of different lipid compositions. Representative images. The lipid composition is DOPC:DSPC (1:1). The predominant phases are stated at the right hand of the pictures. The left-hand and right-hand columns correspond respectively to control and Aurora™-treated bilayers. Bars: 5 µM A height scale is provided with each image. Black corresponds to the mica support.

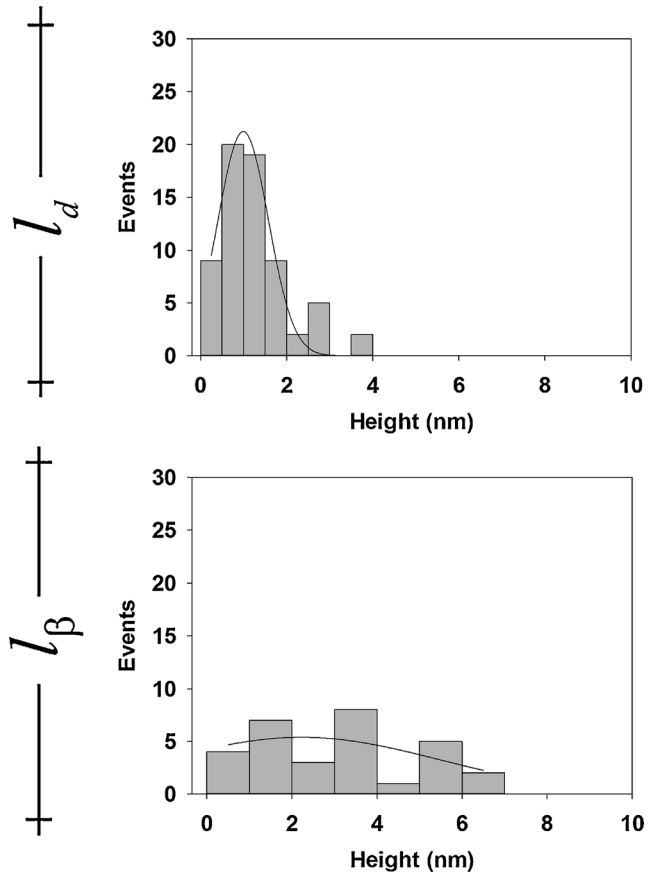

Fig. 4. Statistical analysis of particle height. The maximum height for each particle was measured with respect to the bilayer surface in images as shown in Fig. 3. Top: DOPC:DSPC (l_d). Bottom: DOPC:DSPC ($l_{ß}$).

Table 1
Average heights of the Aurora™ nanoparticles incorporated into supported planar bilayers. Data from Figs. 3 and S3.

Lipid	Height (nm)			
	L_d fluid phase	n	L_β gel phase	n
POPC	2.9 ± 1.25	317	–	
DPPC	–		7.5 ± 0.11	37
DOPC:DSPC	1.2 ± 1.18	70	1.8 ± 1.20	35
DOPC:pSM:Chol	1.6 ± 1.17	144	–	

Average values ± S.D.

throughout image acquisition, they were not dragged nor their apparent height was altered with different tip forces or scan speeds. The results are summarized in Fig. 4, Fig. S7 and Table 1. The average height of the particles is lower for bilayers in the fluid-disordered phase.

3.3. DPH fluorescence polarisation

Lipid bilayer fluidity can be estimated through changes in the polarisation of the fluorescent probe DPH when added to the lipid mixture during liposome preparation. In our case multilamellar vesicles were prepared of compositions POPC, pSM, DPPC and pSM:Chol (6:4), with or without 0.1 mol% Aurora™. The results are summarized in Fig. 5. Aurora™ addition does not give rise to any major changes in bilayer fluidity. However for SM-containing samples addition of Aurora™ causes a slight disordering effect, and an equally small ordering effect is found with PC-containing bilayers. Again the gold nanoparticles appear to

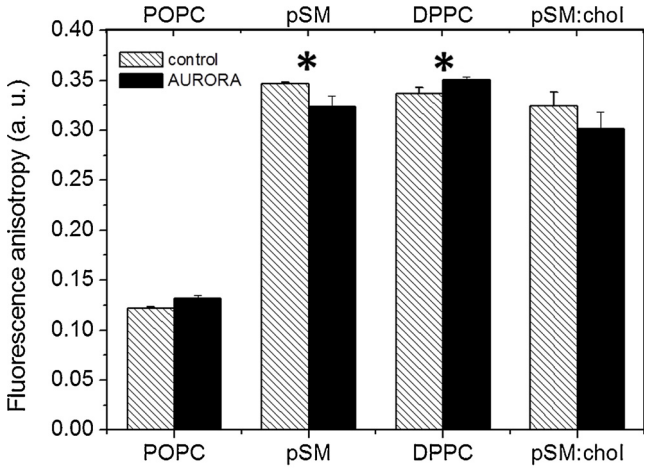

n	6	8	6	10	3	4	3	8
P	0.131		0.00011		0.011		0.066	

Fig. 5. Effect of Aurora™ on bilayer fluidity, measured as DPH fluorescence anisotropy. A higher anisotropy corresponds to a lower fluidity. Main panel: average values of DPH fluorescence anisotropy ± S.D. in bilayers with (black) and without (gray) Aurora™. Lipid compositions are given on top of the main panel. Lower panel: n represents the number of independent measurements, P is the significance parameter according to the Student's t-test, for differences between bilayers plus and minus Aurora™. The asterisks in the main panel point to statistically significant differences ($P < 0.02$).

interact with SM somewhat differently than with PC.

3.4. Cryo-TEM

The incorporation of Aurora™ into POPC bilayers, the ones whose fluidity mimics most closely that of cell membranes, was examined using cryo-TEM. This technique allows the observation of membranes and lipid bilayers under virtually native conditions, free from any dyes or fixative agents. Gold would be expected to increase the contrast of lipid bilayers if incorporated into them. This is indeed the case, as shown in Fig. 6. Panels A and B correspond, respectively, to POPC bilayers in the absence and presence of 0.1 mol% Aurora™. The contrast in the latter case is clearly higher. Fig. S8 D-F show several details at higher magnification. Apart from the enhanced contrast, two features deserve comment. One is that image resolution is enough to allow the observation of single gold clusters in the bilayers (Fig. S8 D,E). In some cases, e.g. Fig. S8 F, a quasi-crystalline lattice of gold clusters has been formed. The second observation is that Aurora™-containing bilayers appear to aggregate, and the flattened surfaces in contact show enhanced contrast, as if the gold nanoparticles would concentrate in such areas (Fig. S8, E,F). In order to obtain some quantitative information of the extent of Aurora™-promoted vesicle aggregation, large unilamellar vesicles of POPC were treated with different amounts of Aurora™, up to 0.4 mol%, and the suspension light scattering measured. Light scattering increases readily with particle size, thus with vesicle aggregation (Goñi and Alonso, 2000). However in our case the increase in light scattering was very small (Fig. S9), suggesting that vesicle aggregation induced by Aurora™ is not a frequent phenomenon under our conditions. A small gallery of POPC vesicles in the absence of gold particles is exhibited in Fig. S10, showing the absence of phenomena that took place in their presence. An additional gallery, including vesicles containing Aurora™, can be seen in Fig. S11.

3.5. Differential scanning calorimetry

Certain lipids, or lipid mixtures, exhibit a gel-to-fluid phase

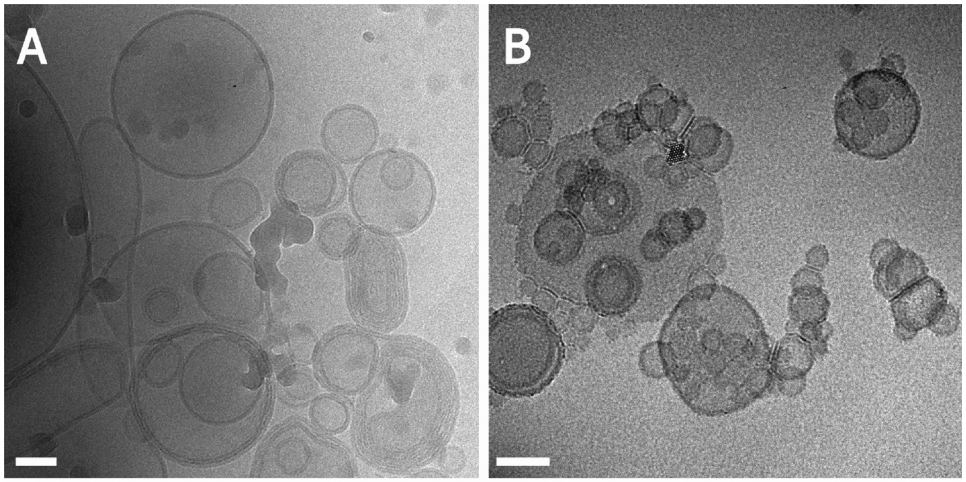

Fig. 6. Cryo-TEM images of vesicles composed of POPC. (A) control. (B) POPC + Aurora™ at 0.1 mol%. Bar = 50 nm.

transition when heated above a given temperature T_m. DSC is a reliable technique for the study of thermotropic phase transitions, and minor changes caused by the presence of other substances are readily detected. DSC thermograms corresponding to DPPC, pSM, and two lipid mixtures used in this study are shown in Fig S12 (Supplementary Material). The two pure lipids and the DOPC:DSPC mixtures, but not the ternary composition DOPC:DSPC:Chol, undergo a cooperative phase transition. These transitions are usually characterized by the transition temperature T_m, the transition width at half-height WHH, and the area under the 'c_p -*vs*-T' curve, i.e. the transition enthalpy ΔH. The corresponding values for the transitions in the absence and presence of Aurora ™ are shown in Table S3 (Supplementary Material). The values are in agreement with data in the literature (Marsh, 2013). Addition of Aurora ™ at the concentration (0.1 mol%) used in the present study hardly alters the thermodynamic parameters of the transition, and no effects are seen that could be attributed to a specific interaction of Aurora ™ with either PC or SM.

4. Discussion

The above results show that, at concentrations appropriate for microscopy observations, Aurora™ does not cause major changes in the physical properties of pure or mixed lipid bilayers, and its presence can be readily detected by AFM and cryo-TEM. Gold nanoparticles absorb light energy and convert it into thermal energy (Link and El-Sayed, 1999). They have thus been suggested to be useful for photothermal therapy, imaging, and photosensitive drug release (Lee et al., 2005; Huang et al., 2007). When integrated in liposomes, gold nanoparticles can give rise to stimuli-sensitive, visible drug carriers (Wu et al., 2008). (Kojima et al. (2009); Chapman, 1975) described the preparation of complexes of liposomes with gold nanoparticles.

Using an alternative approach, we have studied the interaction with liposomes of a derivatised form of Au_{55} (that includes a diacylglycerol molecule) namely Aurora™, that has become commercially available recently. The conjugate lipid-gold structure would permit a more specific targeting to the membrane bilayer, thus increasing the potency of the gold-labeled liposomes. An important initial control was carried out using confocal microscopy of GUV with and without Aurora™ (Figs. 1, S3). The data showed that the presence of the gold nanoclusters did not alter the physical state of the lipids in the membrane (l_d, $l_ß$, l_o), nor did they shift the equilibrium between coexisting domains ($l_ß$ + l_d, l_o + l_d), at least in any markedly detectable way. This is a crucial point to be noted for the practical applications of lipid vesicles labelled with gold nanoparticles. The mild effects of Aurora™ on lipid bilayers were confirmed by our DSC observations (Fig. S12 and Table S3). The narrow endotherm of DPPC or, to a smaller extent, of pSM, reflect the cooperativity of the gel-fluid transition of these lipids (Sot et al., 2008). Any 'impurity' in the bilayer will usually give rise to a widening of the endotherm, a shift in the T_m transition temperature, and a marked change in enthalpy. These are the changes that are typically observed with e.g. cholesterol (Nieva et al., 1989), but none of them are seen in our case. In the equimolar DOPC:DSPC mixture, in which $l_ß$ + l_d phases coexist, Aurora™ could perhaps change the phase equilibrium. However, this does not occur (Fig. S12 C), confirming the innocuous effect of Aurora™ on most lipid bilayers.

Cryo-TEM observations (Figs. 6, S8, S10, S11) are doubly interesting, in that they demonstrate unequivocally the incorporation of the gold nanoparticles to the membranes, and because they do so while increasing notably the sample contrast for the microscopic observations, a property that constitutes the basis for a possible applicability of Aurora™. Also, and in spite of some vesicle aggregation observed (Fig. S8 E, F and S11 B, D, F), the combination of cryo-TEM and light scattering demonstrate that Aurora™-induced vesicle aggregation is a rare phenomenon in our system (Fig. S9). Aggregation is probably a side effect of the diacylglycerol group present in Aurora™ (Viguera et al., 1993; Tian et al., 2008).

AFM observations provide complementary information of the interaction of Aurora™ with lipid bilayers. Aurora ™ did not cause marked changes in SPB morphology (Figs. 2, S4), confirming again that, at least at 0.1 mol%, the gold nanoparticles do not cause observable changes in the lipid phase equilibria. AFM also supplies specific information on the size of the lipid-embedded particles, from measurements of maximum particle height with respect to the lipid plane (Deng et al., 2015; Lentz, 1993). The data in Table 1 show that, at least in the fluid phases, average particle height was in the 1.2–2.9 nm range, with S.D. of the order of 1 nm. The golden particles used in this study are about 1.5 nm in diameter Fig. S2A). Thus it can be safely concluded that, at least under our conditions, Aurora ™ is dispersed in monomeric form within the lipid bilayers, when the latter are in the fluid phase. However with DPPC bilayers at room temperature (in the gel, or $l_ß$ phase) the data in Table 1 may suggest some degree of particle aggregation. The inability to form supported planar bilayers of pSM or pSM/Chol with Aurora also implies indirectly that Aurora has been inserted into the membrane. The significant effects on DOPC:pSM:Chol fluid phase bilayer thickness also point to Aurora being incorporated.

An intriguing, yet not fully explained, phenomenon is that Aurora™ appears to interact with SM somewhat more strongly than with PC. This is suggested by the fact that, in 3-component bilayers, the difference in bilayer thickness between the (higher) less fluid and (lower) more fluid components decreases in the presence of Aurora™ for DOPC:pSM:Chol bilayers, but not for DOPC:DSPC ones (Table S1). Moreover the presence of Aurora in the lipid vesicles hampers bilayer extension and SPB

formation. The latter effect is particularly evident in the pure pSM:Chol samples, for which no SPB could be obtained in the presence of Aurora™ (data not shown). A very different technique, namely DPH fluorescence polarization (Alonso and Goñi, 2018) also indicates some small differences between PC and SM bilayers in their interaction with Aurora™: for SM-containing samples addition of Aurora™ causes a slight disordering effect, and an equally small ordering effect is found with PC-containing bilayers (Fig. 6). These observations could be explained on the basis of the rich network of H-bonds that stabilize the polar headgroups of sphingolipids, but not of glycerophospholipids [40]. However, DSC should be a technique of choice to detect minor effects of a non-bilayer molecule, i.e. Aurora™, on phospholipid bilayers, but no differences are seen in this case (Table S3). It could be proposed that DSC signals arise mainly from melting of the hydrocarbon chains of phospholipids, while interaction with Aurora™ should occur mainly at the headgroup level, but this hypothesis requires further testing.

In conclusion, our data show that Aurora™ particles can be incorporated in monomeric form into fluid bilayers, where they do not exert major interactions with the various lipids. The results confirm the possible application of this form of gold nanoparticles for techniques with therapeutic promise, such as photo-thermal therapy and photo-responsive drug release. In addition, we provide direct proof for the use of Aurora™ as electron microscopy and AFM probes or internal size scale indicators.

Authors contribution

J.S. and S.A.M.N. performed most of the experiments, J.V.B. and A.B.G.-A. provided help with the AFM observations, W.A.S. synthesized Aurora™, D.G. and M.V. carried out the cryo-TEM studies, F.M.G. and A.A. designed the study and wrote the manuscript, all of the above authors helped in the analysis of results.

Conflict of interest

Shengrong Li, S.W. Burgess and W.A. Shaw are employees of Avanti Polar Lipids. The other authors claim no conflicts of interest.

Acknowledgements

This work was supported in part by the Spanish Ministry of Economy (grant No. BFU 2015–66306-P) and by the Basque Government [(grants No. IT-849-13 (F.M.G.) and No. IT838-13 (A.A.)]. A.B.G.-A. was a postdoctoral fellow, supported by the University of the Basque Country.

Appendix A. Supplementary data

Supplementary material related to this article can be found, in the online version, at doi:https://doi.org/10.1016/j.chemphyslip.2018.11.007.

References

Schmid, G., Bäumle, M., Beyer, N., 2000a. Ordered two-dimensional monolayers of Au (55) clusters. Angew. Chem. Int. Ed. Engl. 39, 181–183.
Schmid, G., Simon, U., 2005. Gold nanoparticles: assembly and electrical properties in 1-3 dimensions. Chem. Commun. (Camb.) 14, 697–710.
Schmid, G., 2008. The relevance of shape and size of Au55 clusters. Chem. Soc. Rev. 37, 1909–1930.
Schmid, G., Meyer-Zaika, W., Pugin, R., Sawitowski, T., Majoral, J.P., Caminade, A.M., Turrin, C.O., 2000b. Naked Au55 clusters: dramatic effect of a thiol-terminated dendrimer. Chemistry. 6, 1693–1697.
Balasubramanian, R., Guo, R., Mills, A.J., Murray, R.W., 2005. Reaction of Au(55)(PPh(3))(12)Cl(6) with thiols yields thiolate monolayer protected Au(75) clusters. J. Am. Chem. Soc. 127, 8126–8132.
Li, M., Lohmüller, T., Feldmann, J., 2015. Optical injection of gold nanoparticles into living cells. Nano Lett. 15, 770–775.
Murphy, C.J., Gole, A.M., Stone, J.W., Sisco, P.N., Alkilany, A.M., Goldsmith, E.C., 2008. S.C. Baxter. Gold nanoparticles in biology: beyond toxicity to cellular imaging. Acc. Chem. Res. 41, 1721–1730.
Marchesano, V., Hernandez, Y., Salvenmoser, W., Ambrosone, A., Tino, A., Hobmayer, B., de la Fuente, J.M., Tortiglione, C., 2013. Imaging inward and outward trafficking of gold nanoparticles in whole animals. ACS Nano 7, 2431–2442.
Shukla, R., Bansal, V., Chaudhary, M., Basu, A., Bhonde, R.R., Sastry, M., 2005. Biocompatibility of gold nanoparticles and their endocytotic fate inside the cellular compartment: a microscopic overview. Langmuir 21, 10644–10654.
Schmid, G., Kreyling, W.G., Simon, U., 2017. Toxic effects and biodistribution of ultrasmall gold nanoparticles. Arch. Toxicol. 91, 3011–3037.
Daima, H.K., Selvakannan, P.R., Shukla, R., Bhargava, S.K., Bansal, V., 2013. Fine-tuning the antimicrobial profile of biocompatible gold nanoparticles by sequential surface functionalization using polyoxometalates and lysine. PLoS One 8, e79676.
Sharma, T.K., Ramanathan, R., Weerathunge, P., Mohammadtaheri, M., Daima, H.K., Shukla, R., Bansal, V., 2014. Aptamer-mediated' turn-off/turn-on' nanozyme activity of gold nanoparticles for kanamycin detection. Chem. Commun. (Camb.) 50, 15856–15859.
Tomoaia, G., Horovitz, O., Mocanu, A., Nita, A., Avram, A., Racz, C.P., Soritau, O., Cenariu, M., Tomoaia-Cotisel, M., 2015. Effects of doxorubicin mediated by gold nanoparticles and resveratrol in two human cervical tumor cell lines. Colloids Surf. B Biointerfaces 135, 726–734.
Walker, L., Sood, P., Lenardon, M.D., Milne, G., Olson, J., Jensen, G., Wolf, J., Casadevall, A., Adler-Moore, J., Gow, N.A.R., 2018. The viscoelastic properties of the fungal cell wall allow traffic of AmBisome as intact liposome vesicles. MBio. 9 pii: e02383-17.
Kojima, C., Hirano, Y., Yuba, E., Harada, A., Kono, K., 2008. Preparation and characterization of complexes of liposomes with gold nanoparticles. Colloids Surf. B Biointerfaces 66, 246–252.
Leung, S.J., Romanowski, M., 2012. Molecular catch and release: controlled delivery using optical trapping with light-responsive liposomes. Adv. Mater 24, 6380–6383.
Avanti Polar Lipids catalog. https://avantilipids.com/product/550001.
Angelova, M.I., Dimitrov, D.S., 1986. Liposome electroformation. Faraday Discuss. Chem. Soc. 81, 303–311.
Dimitrov, D.S., Angelova, M.I., 1988. Lipid swelling and liposome formation mediated by electric fields. Bioelectrochem Bioenerg. 19, 323–336.
Montes, L.R., Ahyayauch, H., Ibarguren, M., Sot, J., Alonso, A., et al., 2010. Electroformation of giant unilamellar vesicles from native membranes and organic lipid mixtures for the study of lipid domains under physiological ionic-strength conditions. Methods Mol. Biol. 606, 105–114.
Fidorra, M., Duelund, L., Leidy, C., Simonsen, A.C., Bagatolli, L.A., 2006. Absence of fluid-ordered/fluid-disordered phase coexistence in ceramide/POPC mixtures containing cholesterol. Biophys. J. 90, 4437–4451.
McConnell, H.M., Watts, T.H., Weis, R.M., Brian, A.A., 1986. Supported planar membranes in studies of cell-cell recognition in the immune system. Biochim. Biophys. Acta 864, 95–106.
Goñi, F.M., Alonso, A., Bagatolli, L.A., Brown, R.E., Marsh, D., Prieto, M., Thewalt, J.L., 2008. Phase diagrams of lipid mixtures relevant to the study of membrane rafts. Biochim. Biophys. Acta 1781, 665–684.
Collado, M.I., Goñi, F.M., Alonso, A., Marsh, D., 2005. Domain formation in sphingomyelin/cholesterol mixed membranes studied by spin-label electron spin resonance spectroscopy. Biochemistry 44, 4911–4918.
Sot, J., Ibarguren, M., Busto, J.V., Montes, L.R., Goñi, F.M., Alonso, A., 2008. Cholesterol displacement by ceramide in sphingomyelin-containing liquid-ordered domains, and generation of gel regions in giant lipidic vesicles. FEBS Lett. 582, 3230–3236.
Goñi, F.M., Alonso, A., 2000. Spectroscopic techniques in the study of membrane solubilization, reconstitution and permeabilization by detergents. Biochim. Biophys. Acta 1508, 51–68.
Marsh, D., 2013. Handbook of Lipid Bilayers. CRC Press, Boca Raton, FA, USA.
Link, S., El-Sayed, M.A., 1999. Size and temperature dependence of the plasmon absorption of colloidal gold nanoparticles. J. Phys. Chem. B 103, 4212–4217.
Lee, J., Govorov, A.O., Kotov, N.A., 2005. Nanoparticle assemblies with molecular springs: a nanoscale thermometer. Angew. Chem. Int. Ed. Engl. 44, 7439–7442.
Huang, X., Jain, P.K., El-Sayed, I.H., El-Sayed, M.A., 2007. Gold nanoparticles: interesting optical properties and recent applications in cancer diagnostics and therapy. Nanomedicine Lond. (Lond) 2, 681–693.
Wu, G., Mikhailovsky, A., Khant, H.A., Fu, C., Chiu, W., Zasadzinski, J.A., 2008. Remotely triggered liposome release by near-infrared light absorption via hollow gold nanoshells. J. Am. Chem. Soc. 130, 8175–8177.
Kojima, C., Hirano, Y., Kono, K., 2009. Preparation of complexes of liposomes with gold nanoparticles. Methods Enzymol. 464, 131–145.
Chapman, D., 1975. Phase transitions and fluidity characteristics of lipids and cell membranes. Q. Rev. Biophys. 8, 185–235.
Nieva, J.L., Goñi, F.M., Alonso, A., 1989. Liposome fusion catalytically induced by phospholipase C. Biochemistry 28, 7364–7367.
Viguera, A.R., Mencía, M., Goñi, F.M., 1993. Time-resolved and equilibrium measurements of the effects of poly(ethylene glycol) on small unilamellar phospholipid vesicles. Biochemistry 32, 3708–3713.
Tian, F., Qian, X., Villarrubia, J.S., 2008. Blind estimation of general tip shape in AFM imaging. Ultramicroscopy 109, 44–53.
Deng, W., Zhang, G.M., Murphy, M.F., Lilley, F., Harvey, D.M., Burton, D.R., 2015. Analysis of dynamic cantilever behavior in tapping mode atomic force microscopy. Microsc. Res. Tech. 78, 935–946.
Lentz, B.R., 1993. Use of fluorescent probes to monitor molecular order and motions within liposome bilayers. Chem. Phys. Lipids 64, 99–116.
Alonso, A., Goñi, F.M., 2018. The physical properties of ceramides in membranes. Annu. Rev. Biophys. 47, 633–654.